IAC–25–D1,6,7,x101065

A Multiparametric Programming Approach to Sensitivity Analyses of Exploration Campaign Infrastructure Deployment and Logistics

Nicholas Gollins*[a] and Koki Ho[a]

[a] *Georgia Institute of Technology, Atlanta, Georgia, United States, 30332, ngollins3@gatech.edu*

* *Corresponding author*

Abstract

This paper presents a multiparametric linear programming (mpLP) approach to studying the sensitivity of space exploration logistics plans to uncertainties in the designs of the involved systems. Complex space exploration campaigns are planned far in advance of their expected operational periods and typically require the development of purpose-built systems such as vehicles, habitats, in-situ resource utilisation infrastructure, and scientific equipment. These systems are designed to meet the requirements of the exploration program's plan, but in reality, the coupling between the systems and their requirements is bi-directional. The time and method of the delivery of payloads to their required locations is determined by the payloads' properties and vice-versa: the payloads' designs are constrained by the logistics plan. As a result, the logistics and vehicle designs are prone to over-optimisation and lack robustness to changes during development. Whilst stochastic optimisation offers a solution to this problem, it requires an accurate statistical knowledge of the uncertainties and can nevertheless lead to pessimistic design choices. It would be more useful to a mission planner to understand exactly how the mission design changes as a function of the uncertain parameters. Traditional sensitivity analysis looks at how an optimal solution changes with small perturbations to the problem parameters, whilst parametric programming seeks to understand the values of the optimisation objective and the basic variables across the full range that the problem parameters could take. Through a series of case studies, this paper demonstrates how formulating exploration campaign designs as mpLP problems enables a more rigorous understanding of the coupling between programmatics and system design, and can help mission planners set consistent requirements on both the mission and the systems.

Nomenclature

A	Generic LP constraint coefficient matrix
$\boldsymbol{b}$	Generic LP constraint right-hand side
$\boldsymbol{c}$	Generic LP cost vector
f	Generic optimisation objective function
F	RHS-mpLP constraint-parameter mapping matrix
I_{sp}	Specific impulse
m	Mass
P	LHS-mpLP constraint-variable-parameter mapping tensor
Q	Einstein summation of P over the parameter dimension
t	Time
$\boldsymbol{x}$	Generic optimisation variables
Z	Propellant mass fraction
Δv	Change in velocity
$\boldsymbol{\theta}$	Generic mpLP parameters
μ	ISRU infrastructure maintenance supply rate requirement
ρ	Rate of propellant production from ISRU
σ	Crew supply consumption rate

Subscripts:

A	Active constraint set
L	Lower bound
NA	Inactive constraint set
U	Upper bound

Superscripts:

crew	Crew mass
dry	Vehicle dry (structural) mass
ISRU	ISRU propellant-production infrastructure mass
m	Maintenance supply mass
prop	Propellant mass
s	Crew consumable supply mass

Acronyms/Abbreviations

CR	Critical region
ISRU	*In-situ* resource utilisation
LHS	Left-hand side
LP	Linear Program
mpLP	Multi-Parametric Linear Program
RHS	Right-hand side

1. Introduction

Future crewed deep space exploration missions are likely to involve complex logistics, requiring more supplies and infrastructure than can be delivered in a single launch with the crew. Accordingly, such multi-mission space logistics campaign plans present challenging modelling, design, and optimization problems. The movement of space vehicles and their payloads necessary to fulfil mission requirements can be addressed deterministically using graph-based network flow methods [1–6], and campaign infrastructure systems can be optimized concurrently with the logistics [7–10].

In reality, any model of a future mission plan, architecture, or system, involves a degree of uncertainty. Space mission designs can be optimized with consideration to the uncertainties in order to find solutions of greater robustness; there are a variety of methods by which to achieve this, depending on the type of uncertainty and how it materialises in the specific application. Downs *et al.* presented an overview of the sources and types of uncertainty relevant to the planning of future space missions [11]. Some examples from the literature of space mission optimization under uncertainty include multi-stage stochastic programming for logistics and system design [12]; the use of reinforcement learning for space mission and system design under system uncertainty [13]; mission scheduling under launch uncertainty via stochastic programming [14] and stochastic metaheuristic optimization [15]. More broadly in space systems design, system-of-systems coupling uncertainty has been handled through portfolio management, e.g. [16].

This study is concerned with multi-mission exploration logistics under mission design and system performance uncertainties. This kind of problem can be addressed via multi-stage stochastic programming, which works with expected values of unknown model parameters or outcomes; chance-constrained optimisation, which introduces some reliability requirement as a model constraint; or by robust optimization, which works with worst-case scenarios. However, all of these approaches have their drawbacks - optimization with expected values does not guarantee feasibility, and chance-constrained or robust-optimization typically produces a sub-optimal design. From an exploration program manager's perspective, it would be most useful to understand how the optimal solution varies as a function of the potential realizations of the uncertain parameters. This class of problem is the subject of *parametric programming* [17].

Parametric (or multi-parametric) programming is the methodology surrounding the study of how the optimal solutions of linear or quadratic optimization problems vary depending on their model parameters. In addition to the calculation of optimal solutions to the problem, the methodology aims to identify the "critical regions" of the problem; the regions within which changes to the input parameters do not affect the high-level decisions made in the optimal solution. In the context of space mission design, this would tell the manager the limits of the parameter realizations at which they must make a discrete change in their decision making. Consequently, this information could be used to establish system requirements; for example, if a particular payload's mass breaches some upper limit that triggers a large, discrete change in the optimal mission plan, this would justify imposing an upper bound mass requirement on that payload.

The following paper is organised as follows: first, we introduce the relevant theory from multi-parametric linear programming (mpLP) in Section 2. In Section 3, we discuss the adaptation and extension of a geometric mpLP algorithm. Finally, in Section 5, we apply the method to a two-mission lunar exploration campaign, featuring a pre-deployment mission of infrastructure and supplies followed by an out-and-back crewed mission.

2. Theory

2.1 Multi-Parametric Linear Programming

The general form of a linear programming (LP) minimization problem with n variables and m constraints is given in Eq. 1.

$$\begin{aligned} \min_{\boldsymbol{x}} \ & f(\boldsymbol{x}) = \boldsymbol{c}^T \boldsymbol{x} \\ \text{s.t. } & A\boldsymbol{x} \geq \boldsymbol{b} \end{aligned} \tag{1}$$

Where $\boldsymbol{x} \in \mathbb{R}^n, \boldsymbol{b} \in \mathbb{R}^m, A \in \mathbb{R}^{m \times n}$. For an optimal solution $\boldsymbol{x}^*$, there will be a set of active constraints, and a set of inactive constraint. These are denoted by the subscripts A and NA respectively:

$$\begin{aligned} A_{\text{NA}}\boldsymbol{x}^* &\geq \boldsymbol{b}_{\text{NA}} \\ A_{\text{A}}\boldsymbol{x}^* &= \boldsymbol{b}_A \end{aligned} \tag{2}$$

A property of non-degenerate LPs is that there are as many active constraints as there are variables, i.e. $A_{\text{A}} \in \mathbb{R}^{n \times n}, A_{\text{NA}} \in \mathbb{R}^{(m-n) \times n}$.

A *parametric* linear program contains variable or uncertain terms in the cost $\boldsymbol{c}$, or constraint terms A or $\boldsymbol{b}$. These uncertain terms are referred to as *parameters*. The general (or sometimes called global) multi-parametric linear program is defined in Eq. 3. The general mpLP features an arbitrary p of parameters θ in any of the costs or constraints.

$$\begin{aligned} \min_{\boldsymbol{x}} \; & f(\boldsymbol{x}, \boldsymbol{\theta}) = \boldsymbol{c}(\boldsymbol{\theta})^T \boldsymbol{x} \\ \text{s.t. } & A(\boldsymbol{\theta})\boldsymbol{x} \geq \boldsymbol{b}(\boldsymbol{\theta}) \end{aligned} \quad [3]$$

where $\boldsymbol{\theta} \in \mathbb{R}^p, \boldsymbol{\theta}_L \leq \boldsymbol{\theta} \leq \boldsymbol{\theta}_U$.

Whilst a traditional optimisation problem seeks only to find the optimal set of variables subject to the fully determined problem, mpLP methods seek to understand how the optimal variable values change across the full range of the parameters. The result is the identification of a set of *critical regions* (CRs); regions within which the set of non-zero (basis) variables remains the same (equivalently, the regions where the set of active constraints remains the same).

The general problem is the most challenging to solve. However, depending on the optimisation problem in question, it is often possible to partition the parameters that appear in the different parts of the problem. Cost parameters are the most easily addressed and are not the subject of this work. Right-hand side (RHS) mpLP problems address the parameters appearing on the right-hand side of the constraints, $\boldsymbol{b}(\boldsymbol{\theta})$, and left-hand side (LHS) mpLP problems address the parameters appearing in the constraint coefficient matrix $A(\boldsymbol{\theta})$. The generic RHS- and LHS-mpLP problems are defined in Eqs. 4 - 5 respectively [18, 19].

$$\begin{aligned} \min_{\boldsymbol{x}} \; & f(\boldsymbol{x}) = \boldsymbol{c}^T \boldsymbol{x} \\ \text{s.t. } & A\boldsymbol{x} \geq \boldsymbol{b}(\boldsymbol{\theta}) \end{aligned} \quad [4]$$

$$\begin{aligned} \min_{\boldsymbol{x}} \; & f(\boldsymbol{x}) = \boldsymbol{c}^T \boldsymbol{x} \\ \text{s.t. } & A(\boldsymbol{\theta})\boldsymbol{x} \geq \boldsymbol{b} \end{aligned} \quad [5]$$

The following subsections 2.2 and 2.3 outline the process of defining the critical regions for RHS- and LHS-mpLPs respectively. Sections 2.4 and 2.5 provide a short discussion on degeneracy and edge cases and their relevance specifically to typical space mission design problems. For in-depth discussions of these topics, we refer the reader to the extensive literature, e.g. [20–24].

2.2 Solving RHS-mpLPs

The method for identifying CRs of RHS problems presented here was first developed by Borelli *et al* [20]. This section provides a summary of the necessary results, but the reader is referred to the original paper for derivations and discussion of edge-cases.

First, we more precisely formulate the problem of Eq. 4 by defining the RHS as $\boldsymbol{b}(\boldsymbol{\theta}) = \boldsymbol{b} + F\boldsymbol{\theta}$, where $F \in \mathbb{R}^{m \times p}$ is a matrix that maps the parameters onto the constraints. For some realisation of the parameters $\boldsymbol{\theta}_0$, Eq. 2 becomes Eq. 6

$$\begin{aligned} A_{\text{NA}}\boldsymbol{x}^* &\geq \boldsymbol{b}_{\text{NA}} + F_{\text{NA}}\boldsymbol{\theta}_0 \\ A_{\text{A}}\boldsymbol{x}^* &= \boldsymbol{b}_A + F_{\text{A}}\boldsymbol{\theta}_0 \end{aligned} \quad [6]$$

The CR is the region in $\boldsymbol{\theta}$-space for which Eq. 6 holds. Within the CR, the optimal variable values as a function of the parameters are given by Eq. 7. This leads to Eq. 8, which defines the polytope that bounds the CR about $\boldsymbol{\theta}_0$.

$$\boldsymbol{x}^*(\boldsymbol{\theta}) = A_{\text{A}}^{-1}(\boldsymbol{b}_A + F_{\text{A}}\boldsymbol{\theta}) \quad [7]$$

$$A_{\text{NA}}A_{\text{A}}^{-1}(\boldsymbol{b}_A + F_{\text{A}}\boldsymbol{\theta}) - \boldsymbol{b}_{\text{NA}} - F_{\text{NA}}\boldsymbol{\theta} \geq 0 \quad [8]$$

Finally, the optimal objective f^* is found by evaluating the product of the cost vector and Eq. 7:

$$f^*(\boldsymbol{\theta}) = \boldsymbol{c}^T A_{\text{A}}^{-1}(\boldsymbol{b}_A + F_{\text{A}}\boldsymbol{\theta}) \quad [9]$$

It is important to note that it is possible to refer to Eq. 9 as the *optimal* objective because, for RHS problems, $\boldsymbol{\theta}$ appears only in the objective of the dual problem and therefore does not affect the dual feasibility of the basis. Since both the primal and the dual problems remain feasible within the CR, it follows that the solution remains optimal.

2.3 Solving LHS-mpLPs

The overall process for finding the CRs of the LHS problem follows the same key steps as the RHS problem. First, we again start by more precisely formulating the LHS-mpLP problem by defining $A(\boldsymbol{\theta}) = A + Q$, where $Q = \sum_{i=0}^{p} P_i\boldsymbol{\theta}_i$ is the Einstein summation [25] of the tensor $P \in \mathbb{R}^{m \times n \times p}$ over the parameter dimension. The term $P_{i,j,k}$ adds the parameter θ_k to the constraint coefficient $A_{i,j}$.

Now, Eq. 2 becomes Eq. 10.

$$\begin{aligned} \left(A_{\text{NA}} + Q_{\text{NA}}\boldsymbol{\theta}\right)\boldsymbol{x}^* &\geq \boldsymbol{b}_{\text{NA}} \\ \left(A_{\text{A}} + Q_{\text{A}}\boldsymbol{\theta}\right)\boldsymbol{x}^* &= \boldsymbol{b}_A \end{aligned} \quad [10]$$

Again, this leads to the optimal variable values, critical region bounds, and objective values, given respectively in Eqs. 11 - 13.

$$\boldsymbol{x}^*(\boldsymbol{\theta}) = \left(A_{\text{A}} + Q_{\text{A}}\boldsymbol{\theta}\right)^{-1}\boldsymbol{b}_A \quad [11]$$

$$\left(A_{\text{NA}} + Q_{\text{NA}}\boldsymbol{\theta}\right)\left(A_{\text{A}} + Q_{\text{A}}\boldsymbol{\theta}\right)^{-1}\boldsymbol{b}_A - \boldsymbol{b}_{\text{NA}} \geq 0 \quad [12]$$

$$f(\boldsymbol{\theta}) = \boldsymbol{c}^T\left(A_{\text{A}} + Q_{\text{A}}\boldsymbol{\theta}\right)^{-1}\boldsymbol{b}_A \quad [13]$$

Unlike with RHS-mpLP problems, it cannot be said with certainty that Eq. 13 remains optimal throughout the CR. This is because parameters in the constraint matrix appear also in the constraint matrix of the dual problem and can therefore impact the feasibility of the basis in the dual problem. If the basis becomes dual infeasible under a certain $\boldsymbol{\theta}$, it becomes sub-optimal for the primal problem.

2.4 Degeneracy

Eqs. 6 - 13 all assume that the mpLP is not degenerate. That is to say, there are no redundant constraints in the optimal basis. A constraint is considered to be redundant if its removal does not change the shape of the feasible region. Particularly relevant to mpLP problems are *weakly redundant* constraints. From [26], a weakly redundant constraint is one that is tight at the optimal solution, but its removal does not change the solution.

Redundant constraints appear and disappear as parameters on either side of the constraints vary. The following Section 3.3 discusses the specific method by which degenerate cases are handled algorithmically. In this Theory section, though, it is necessary to acknowledge the impact of potential degeneracies on the solution of the mpLP.

Consider two adjacent CRs. By definition, each CR has a unique set of active constraints associated with it. As stated in Section 2.1, the optimal solution of a non-degenerate LP will have n active constraints. In the present of redundant constraints, it is possible for $> n$ constraints to be active. If, in one of the CRs, a redundant constraint is in the active constraint set of its neighbour, and vice-versa, we will observe overlap between the two CRs.

2.5 Edge Cases

When a set of constraints A_{A} becomes active only when a subset of parameters takes an exact value, the corresponding CR will be lower-dimensional in $\boldsymbol{\theta}$-space. For example, for a two-parameter problem ($\boldsymbol{\theta} = [\theta_1, \theta_2]^T$), the following edge cases are possible:

1. A_{A} is active only when $a\theta_1 + b\theta_2 = c$, where a, b, c are some constants, the resulting CR will be a line in $\boldsymbol{\theta}$ space.

2. A_{A} is active only when $\theta_1 = a$ and $\theta_2 = b$, the resulting CR will be a point in $\boldsymbol{\theta}$-space.

However, such edge cases have little relevance to real-world design problems, because they require a parameter to take an exact value. In reality, it is impossible to achieve a design parameter *exactly*; there is always some tolerance. Therefore, the design decisions corresponding to the edge case would always be infeasible or sub-optimal in practice. For the remainder of this paper, we will neglect potential edge cases.

3. Method

3.1 RHS-mpLP Algorithm

The procedure for solving RHS-mpLP problems is as follows:

1. Solve Eq. 4 for some initial set of parameters $\boldsymbol{\theta} = \Theta_0$.

2. Calculate the polytope formed by Eq. 8. Polytope management for the RHS problems was handled using the pycddlib Python package [27, 28].

3. Let Θ_i be the central point of the i^{th} edge of the polytope. Take a small step $d\boldsymbol{\theta}_i$ in the direction away from the polytope, perpendicular to the edge.

4. Repeat steps 1-3, replacing $\boldsymbol{\theta} = \Theta_0$ with $\boldsymbol{\theta} = \Theta_i + d\boldsymbol{\theta}_i$ for each edge i. If the problem is infeasible for the current $\boldsymbol{\theta}$, move on to the next edge.

5. Stop when all remaining edges already exist in regions that have been evaluated or are outside the parameter bounds.

An example of how the algorithm proceeds for a simple RHS-mpLP with two parameters is given in Figure 1. The green points indicate tested parameters that produce feasible LPs, and red points indicate tested parameters that produce infeasible LPs. Shaded regions indicate the CR around their respective feasible parameters. The unshaded regions indicate infeasible parameters.

3.2 LHS-mpLP Algorithm

The solution procedure for LHS-mpLP problems is more difficult to automate using the methods presented here than for RHS problems. Primarily, this is because Eq. 12 is non-linear in $\boldsymbol{\theta}$, making it challenging to formulate an expression for the polytope formed in $\boldsymbol{\theta}$-space. Charitopoulos *et al.* [29] employed symbolic manipulation software for solving this problem, but this approach does not scale well.

Therefore, instead of precisely calculating the polytope of the CR, we simply calculate the residual of Eq. 12 for samples across the entire parameter space. The CR is formed by the samples for which Eq. 12 is satisfied. This algorithm is summarised as follows:

1. Create a grid of samples across the parameter space.

2. Solve Eq. 5 for some initial set of parameters $\boldsymbol{\theta} = \Theta_0$.

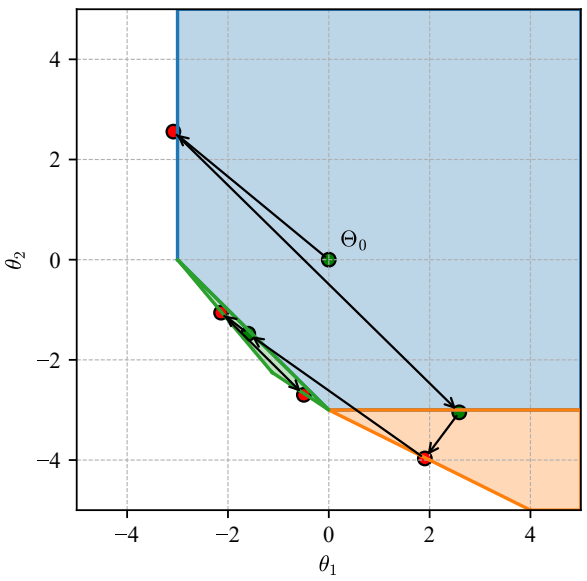

Fig. 1. Example of the RHS-mpLP solution procedure. Dots indicate the parameter values for which the LP was solved; green indicates feasible parameters, red indicates infeasibility. Shaded regions indicate the CRs associated with the enclosed parameter sample.

3. Calculate the residual of Eq. 12 for all parameter samples. Assign samples that satisfy Eq. 12 to the current CR.
4. Repeat steps 2 - 3 for some subset of parameter samples Θ_i.
5. Evaluate Eq. 13 across each critical region. Remove overlapping regions from CRs that are found to be sub-optimal within the overlap.
6. Stop when the LP has been evaluated under all parameter samples.

The selection of the subset of parameters for which to solve Eq. 5 in Step 4 of the algorithm is somewhat difficult to automate, and requires at least some manual exploration of the sample space to build an understanding of the CRs.

A demonstration of the LHS-mpLP solution procedure is shown in Figure 2 for a subset of the sampled points. The green points indicate the sampled parameter values, and the coloured area shows the CR about the sampled point. Note, unlike the RHS example, there is overlap between the CRs: the blue region shares parameter space with both the orange and the green regions. This is due to the points discussed in Section 2.3; that LHS solutions can become sub-optimal within a CR. Referring to Figure 2, the LP was solved under three parameters: $\mathbf{\Theta}_0, \mathbf{\Theta}_1$, and $\mathbf{\Theta}_2$. Call the blue, orange, and green regions CR_0, CR_1, and CR_2 respectively, let their active constraint sets be $A_{A,0}, A_{A,1}$, and $A_{A,2}$, and let the objective under those active constraints be f_0, f_1, and f_2. Solving for $\mathbf{\Theta}_0$ discovered CR_0, but $\mathbf{\Theta}_0$ is also enclosed by CR_1. From this, we can know that $\mathbf{\Theta}_0$ satisfies Eq. 12 for both CR_0 and CR_1, but $f_0(\mathbf{\Theta}_0) < f_1(\mathbf{\Theta}_0)$. Similarly, solving the LP for $\mathbf{\Theta}_2$ discovered CR_2, but $\mathbf{\Theta}_2$ is also enclosed by CR_0. Therefore, we also know that $\mathbf{\Theta}_2$ satisfies Eq. 12 under both $A_{A,0}$ and $A_{A,2}$, but $f_2(\mathbf{\Theta}_2) < f_0(\mathbf{\Theta}_2)$.

It is worth noting that this method for solving LHS-problems is also applicable to combined RHS- and LHS-problems by combining Eqs. 7 - 9 with Eqs 11 - 13. For simplicity, the scope of the case study is limited to addressing each of these problem classes individually.

3.3 A Note on Matrix Inverses

As mentioned in Section 2.1, A_A is square for non-degenerate and bounded LPs. For such cases, there is no issue with taking the inverse required in Eq. 2. However, once $\boldsymbol{\theta}$ has been incorporated into the expression, it is possible (and even likely) that A_A can become singular or non-square. For this reason, the methods discussed in Sections 3.1 and 3.2 replace the inverses in Eqs. 7 - 9 and 11 - 13 with pseudo- (also known as generalised, or Moore-Penrose) inverses [30], denoted by †. The pseudo-inverse has the following properties:

- If A is square and non-singular, $A^\dagger = A^{-1}$
- If A non-invertible and $Ax = b$ has no exact solution, then $x = A^\dagger b$ is the least-squares solution.
- If A non-invertible and $Ax = b$ has multiple solutions, then $x = A^\dagger b$ is the minimum-norm solution.

In this work, the pseudo-inverse is largely used for algorithmic robustness and computation speed. The alternative approach would be to check for degeneracy after each LP solve, and perform a Gaussian elimination in order to find an invertible matrix. However, this is extremely time-consuming for large problems, and does not solve the problem of encountering singularities as $\boldsymbol{\theta}$ varies. Therefore, we instead proceed with the pseudo-inverse and note that the LHS-mpLP results should be interpreted as approximate in the neighbourhoods of parameter-space that result in constraint singularity.

4. Case Study Definition

4.1 Overview

This paper aims to demonstrate the effectiveness of mpLP methods in quantifying the impacts of uncertainties

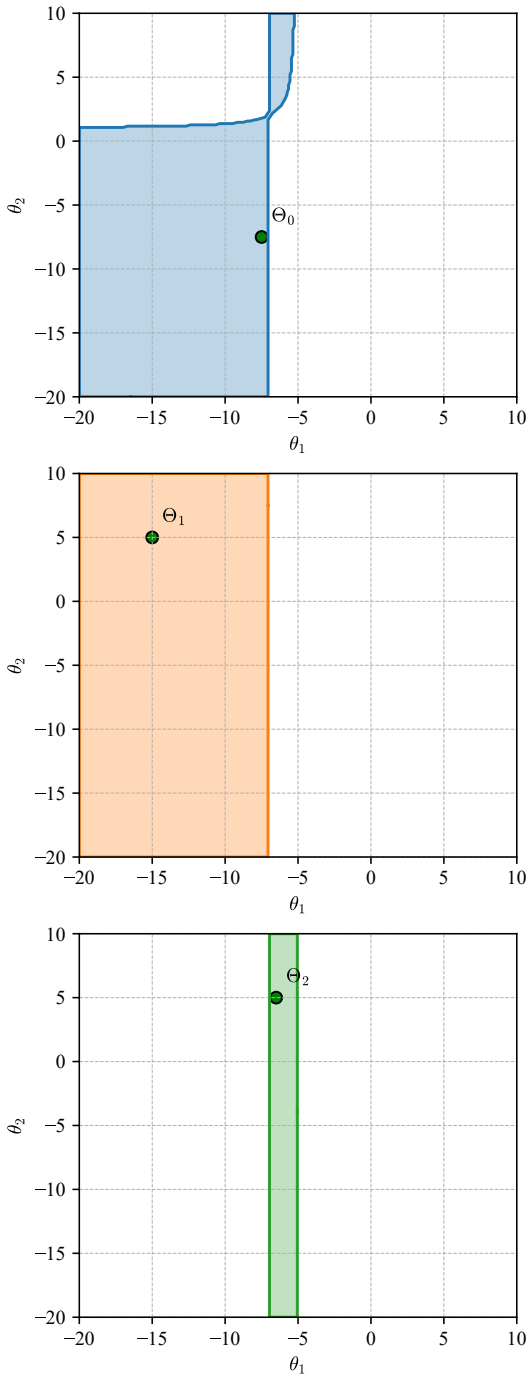

Fig. 2. Example of the LHS-mpLP solution procedure. Green points indicate the parameter values for which the LP was solved. Infeasible parameter samples have not been included for brevity. Shaded regions indicate the CRs associated with the enclosed parameter sample. Due to significant overlap between the CRs, each CR has been plotted on its own axis for clarity.

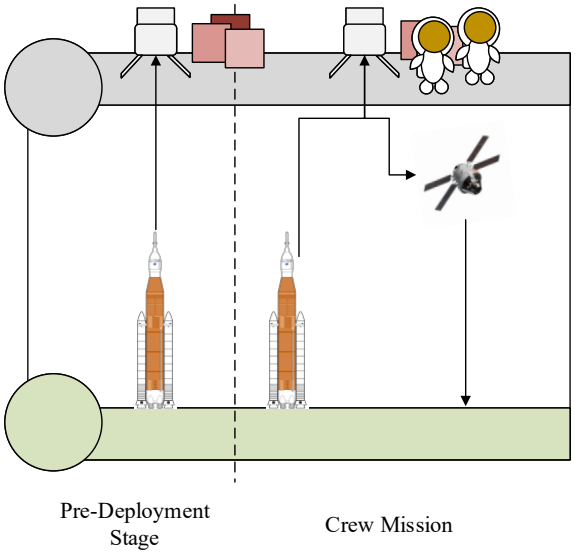

Fig. 3. Diagram of the case study mission.

surrounding staged deployment problems on the initial decisions to be made by the mission planner. To do this, we will consider the staged deployment of a lunar surface outpost as a case study. This section provides a qualitative description of the case study, and the following Section 4.2 defines the variables, constant parameters, objective and constraint of the case study's design optimisation problem. Finally, Sections 4.3 - 4.5 set up the specific mpLPs that we will study. In all parametric studies, we will consider the variation of two parameters at a time for the simplicity of communicating the results. The methods demonstrated can be extended to any number of parameters.

We consider a two-stage deployment of a crewed lunar surface exploration mission. In the first stage, an uncrewed mission is launched to the lunar surface with the purpose of pre-deploying payloads (such as a habitat, rover etc), supplies, and ISRU infrastructure for propellant production. The second stage consists of two legs: the outbound leg is the launch of the crew, the return vehicle, and further supplies and payloads. The final leg is the return of the crew from the lunar surface, returning only with the supplies necessary for the return trip. Figure 3 illustrates the case study mission..

4.2 LP Formulation

The decision that the mission planner must make in this case study is: how much propellant, supplies, and ISRU infrastructure should be launched with each stage of the mission? Therefore, the variables are as follows:

- $m_i^{\text{prop}} \in \mathbb{R}^3$: the amount of propellant to be used on

each of the 3 mission legs, where i is the leg index.

- $m_i^{\text{s}} \in \mathbb{R}^3$: the mass of crew supplies that are consumed on each of the 3 mission legs.
- $m_i^{\text{m}} \in \mathbb{R}^2$: the mass of maintenance supplies that should be launched on the first and second mission legs, used for making any necessary repairs to the ISRU infrastructure.
- $m^{\text{ISRU}} \in \mathbb{R}$: the mass of ISRU infrastructure to be launched on the first leg of the mission.

The objective of the problem is to minimise the total mass that must be launched from Earth:

$$\min_m \; f(m) = m^{\text{ISRU}} + \sum_{i=0}^{2} m_i^{\text{prop}} + \sum_{i=0}^{1} (m_i^{\text{s}} + m_i^{\text{m}}) \quad [14]$$

The constraints enforce the physics and dynamics of each of the commodities. At this point, a number of parameters are introduced; each will be summarised as they appear. First, propellant consumption must obey the rocket equation:

$$m_0^{\text{prop}} \geq Z_0 \left(m^{\text{ISRU}} + m_0^{\text{m}} + m_0^{\text{s}} + m_0^{\text{dry}} \right) \quad [15]$$

$$m_1^{\text{prop}} \geq Z_1 \left(m_1^{\text{m}} + m_1^{\text{s}} + m_1^{\text{dry}} + m_2^{\text{dry}} + m_2^{\text{prop}} + m^{\text{crew}} \right) \quad [16]$$

$$m_2^{\text{prop}} + \rho(t_{0,1} + t_1 + t_{1,2}) m^{\text{ISRU}} \geq Z_2 \left(m_2^{\text{supplies}} + m_2^{\text{dry}} + m^{\text{crew}} \right) \quad [17]$$

Where Z_i is ratio between propellant mass and final mass after a Δv manoeuvre, given by $Z_i = \exp(\Delta v_i / g_o I_{\text{sp},i}) - 1$. Δv_i is the total Δv required for the i^{th} leg of the mission, and $I_{\text{sp},i}$ is the specific impulse of the vehicle used for the same leg. It is assumed that no staging or payload collection/delivery occurs in between manoeuvres. m_i^{dry} is the dry (structural) mass of the vehicle used on the i^{th} leg. t_i is the time length of leg i, and $t_{i,j}$ is the time *between* legs i and j. In words, $t_{0,1}$ is the time between the pre-deployment mission and the launch of the crewed mission, and $t_{1,2}$ is the time that the crew spends on the lunar surface. t_1 and t_2 are the times spent by the crew travelling between Earth and the lunar surface and *vice-versa*. ρ is the mass of propellant produced per unit mass of ISRU infrastructure per unit time.

Next, there is a lower bound on the mass of ISRU maintenance supplies required proportional to the mass of ISRU infrastructure and the time for which the infrastucture operates:

$$\sum_{i=0}^{1} m_i^{\text{m}} \geq \mu t_{0,1} m^{\text{ISRU}} \quad [18]$$

Where μ is the mass of maintenance supplies per unit mass of ISRU infrastructure per unit time.

Similarly, there are lower bounds on the crew supplies required:

$$\sum_{i=0}^{1} m_i^{\text{s}} \geq \sigma(t_1 + t_{1,2}) + m_2^{\text{s}} \quad [19]$$

$$m_1^{\text{s}} \geq \sigma t_1 \quad [20]$$

$$m_2^{\text{s}} \geq \sigma t_2 \quad [21]$$

Where σ is the mass of supplies required by the crew per unit time.

Finally, we require that all variables be non-negative:

$$\begin{aligned} m_i^{\text{prop}} &\geq 0 \;\; \forall \;\; i \in (0,1,2) \\ m_i^{\text{s}} &\geq 0 \;\; \forall \;\; i \in (0,1,2) \\ m_i^{\text{m}} &\geq 0 \;\; \forall \;\; i \in (0,1) \\ m^{\text{ISRU}} &\geq 0 \end{aligned} \quad [22]$$

In summary, the non-parametric LP is the following:

$$\begin{aligned} &\min \text{ Eq.14} \\ &\text{s.t. Eqs.} 15 - 22 \end{aligned} \quad [\text{LP}]$$

Table 1 outlines the default values for each of the parameters used in the case study.

Table 1. Default parameters values of LP.

Parameters	Value
g_0	9.8 m/s^2
$\Delta v_0, \Delta v_1, \Delta v_2$	2000, 2000, 2000 m/s
$I_{\text{sp},0}, I_{\text{sp},1}, I_{\text{sp},2}$	320, 320, 320 s
$m_0^{\text{dry}}, m_1^{\text{dry}}, m_2^{\text{dry}}$	10000, 10000, 1000 kg
m^{crew}	300 kg
ρ	0.00153 kg / kg infra / day [31]
μ	0.1 kg / kg infra / day
σ	10 kg / day
$t_{0,1}$	365 days
$t_{1,2}$	30 days
t_1, t_2	5, 5 days

4.3 Case Study 1

In this first study, we will analyse the effects of variations in the consumable supplies required by the crew in different parts of the mission. To the RHS of Eq. 19 we add a parameter $-10 \leq \Delta\sigma_1 \leq +90$, representing variation in the supplies required during the surface mission. To the RHS of Eq. 20 we add the parameter $-10 \leq \Delta\sigma_2 \leq +90$, representing a change in the supplies required during the crew's outbound journey to the Moon. Eqs. 19 and 20 become:

$$\sum_{i=0}^{1} m_i^{\mathrm{s}} \geq (\sigma + \Delta\sigma_1)(t_1 + t_{1,2}) + m_2^{\mathrm{s}} \quad [23]$$

$$m_1^{\mathrm{s}} \geq (\sigma + \Delta\sigma_2)t_1 \quad [24]$$

So the RHS-mpLP of Case Study 1 is the following:

$$\begin{aligned} &\min \text{ Eq.14} \\ &\text{s.t. Eqs.} 15-18, 21-24 \\ &\boldsymbol{\theta} = [\Delta\sigma_1, \Delta\sigma_2]^T \end{aligned} \quad [\text{mpLP1}]$$

4.4 Case Study 2

In this second study, we study the effect of uncertain vehicle mass on the optimal solution. Again we introduce two parameters, the first of which represents changes to the masses of the two descent vehicles (which we will assume have the same design), $-9000 \leq \Delta m_d^{\mathrm{dry}} \leq +10000$. The second parameter $-900 \leq \Delta m_a^{\mathrm{dry}} \leq +9000$ represents changes to the mass of the ascent vehicle. Eqs. 15 - 17 become the following:

$$\begin{aligned} m_0^{\mathrm{prop}} \geq Z_0 \big(&m^{\mathrm{ISRU}} + m_0^{\mathrm{m}} + \\ &m_0^{\mathrm{s}} + m_0^{\mathrm{dry}} + \Delta m_d^{\mathrm{dry}}\big) \end{aligned} \quad [25]$$

$$\begin{aligned} m_1^{\mathrm{prop}} \geq Z_1 \Big(&m_1^{\mathrm{m}} + m_1^{\mathrm{s}} + m_1^{\mathrm{dry}} + \Delta m_d^{\mathrm{dry}} + \\ &m_2^{\mathrm{dry}} + \Delta m_a^{\mathrm{dry}} + m_2^{\mathrm{prop}} + m^{\mathrm{crew}}\Big) \end{aligned} \quad [26]$$

$$\begin{aligned} m_2^{\mathrm{prop}} + \rho(t_{0,1} + t_1 + t_{1,2})m^{\mathrm{ISRU}} \geq \\ Z_2 \Big(m_2^{\mathrm{supplies}} + m_2^{\mathrm{dry}} + \Delta m_a^{\mathrm{dry}} + m^{\mathrm{crew}}\Big) \end{aligned} \quad [27]$$

So the RHS-mpLP of Case Study 2 is the following:

$$\begin{aligned} &\min \text{ Eq.14} \\ &\text{s.t. Eqs.} 18-22, 25-27 \\ &\boldsymbol{\theta} = \left[\Delta m_d^{\mathrm{dry}}, \Delta m_a^{\mathrm{dry}}\right]^T \end{aligned} \quad [\text{mpLP2}]$$

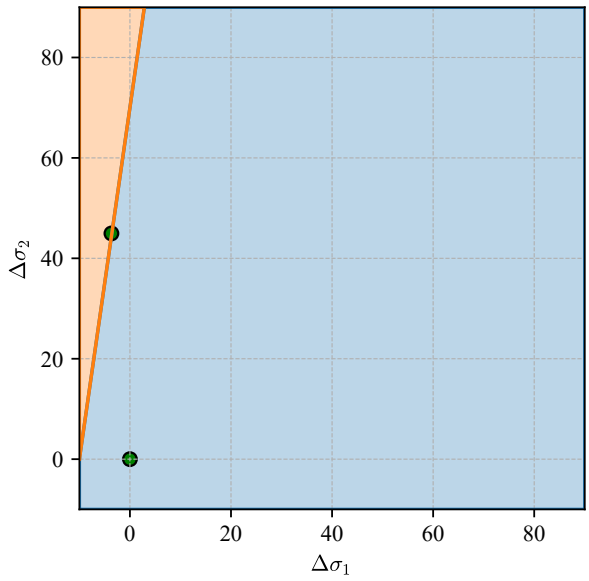

Fig. 4. CRs of Case Study 1. Green points indicate the parameters for which mpLP1 was solved. The blue region is CR_0, the orange is CR_1.

4.5 Case Study 3

In the third and final study we will consider variations to the LHS parameters ρ and μ, representing uncertainty surrounding the performance and requirements of the ISRU infrastructure. To Eq. 17 we add a $-0.00153 \leq \Delta\rho \leq +0.1$ parameter:

$$\begin{aligned} m_2^{\mathrm{prop}} + (\rho + \Delta\rho)(t_{0,1} + t_1 + t_{1,2})m^{\mathrm{ISRU}} \\ \geq Z_2 \left(m_2^{\mathrm{supplies}} + m_2^{\mathrm{dry}} + m^{\mathrm{crew}}\right) \end{aligned} \quad [28]$$

And to Eq. 18 we add a $-0.1 \leq \Delta\mu \leq +0.1$ parameter:

$$\sum_{i=0}^{1} m_i^{\mathrm{m}} \geq (\mu + \Delta\mu)t_{0,1}m^{\mathrm{ISRU}} \quad [29]$$

In summary, the LHS-mpLP of Case Study 3 is the following:

$$\begin{aligned} &\min \text{ Eq.14} \\ &\text{s.t. Eqs.} 15-16, 18-22, 28-29 \\ &\boldsymbol{\theta} = [\Delta\rho, \Delta\mu]^T \end{aligned} \quad [\text{mpLP3}]$$

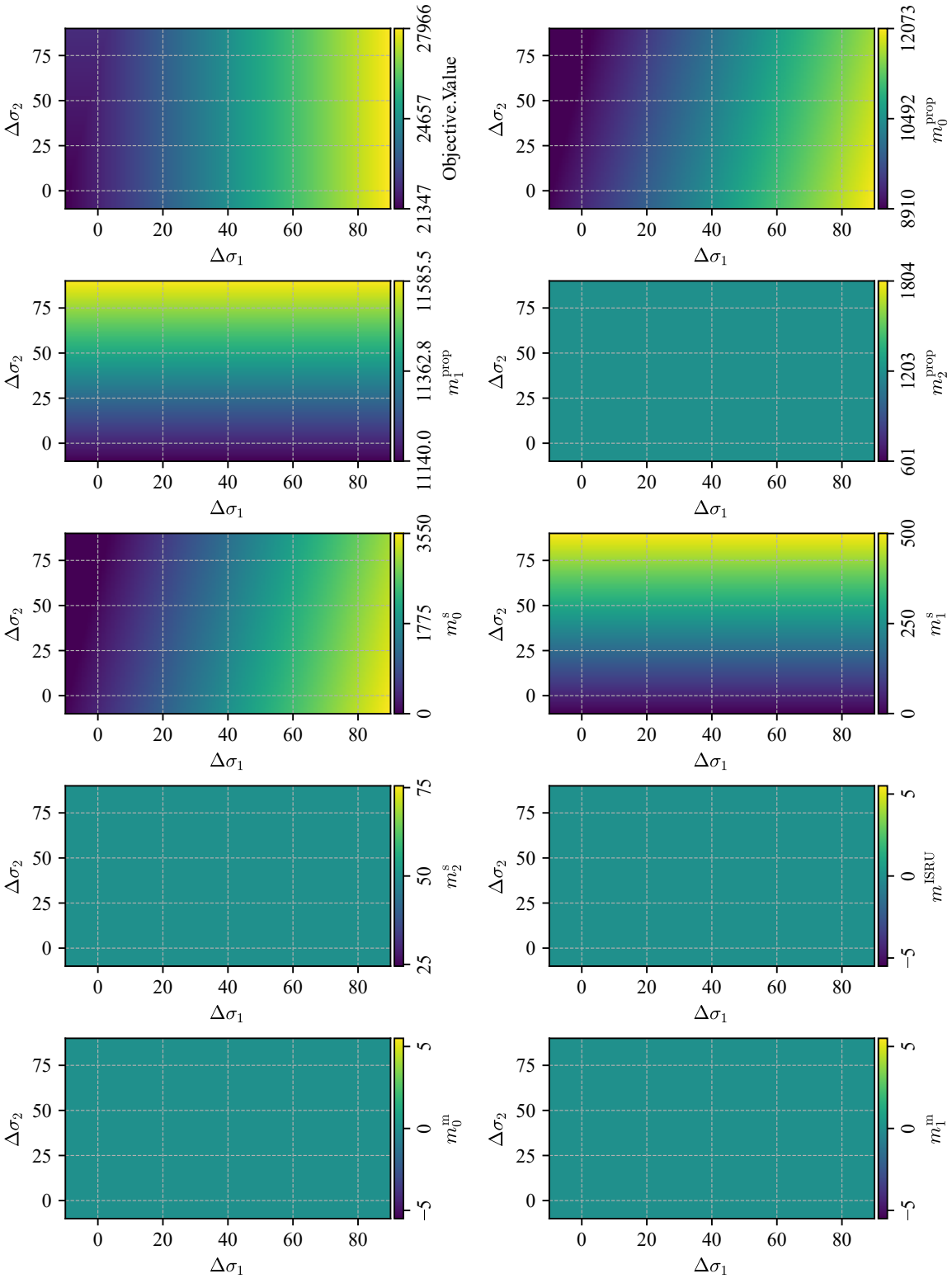

Fig. 5. Objective and variable values as functions of the RHS-parameters of Case Study 1.

5. Results

5.1 Case Study 1

In Case Study 1, two CRs were identified. These are shown in Figure 4. The region containing the baseline case, which we will call CR_0, covers the majority of the parameter space, showing good robustness of the baseline solution. The other region, CR_1, occurs when surface mission supply requirements are very low, and the in-space section of the outbound journey has very high supply requirements.

Figure 5 shows how the optimal objective and variable values vary with the parameters. These results show that the objective is more heavily dependent on the surface mission supply requirements; this makes sense, as the surface mission is the longest stage of the crewed mission.

We can also see that varying the supply requirements in isolation does not affect the ISRU infrastructure, under its baseline design. In this particular case, ISRU infrastructure is simply unused.

The key distinction between the two critical regions is regarding the decision to pre-deploy any crew supplies or not. In the baseline CR_0, crew supplies are indeed pre-deployed, with the exact amount depending on the supply requirements. In CR_1, where surface mission supply requirements are much smaller, the decision to pre-deploy supplies becomes sub-optimal, and the crew carries along all of the required supplies. In this case, the pre-deployment mission would only deliver inert payloads that would be considered non-optional to the mission requirements, such as a crew habitat. Mathematically, such payloads are included in the m_0^{dry} term.

5.2 Case Study 2

As shown in Figure 6, the baseline critical region CR_0 encompasses the entire parameter space in Case Study 2. Whilst this may instictively feel an uninteresting result, this demonstration of a "null" outcome still provides the mission designer with valuable information: their decisions are not influenced by the vehicle masses, in the absence of other parameter variations. Consequently, the vehicle's system mass requirements can be uncoupled from the mission variables at this level of fidelity.

5.3 Case Study 3

Figure 7 shows the variation of the optimal objective and variables with $\Delta\rho$ and $\Delta\mu$. Unlike the Case Studies 1 and 2, the CRs are not plotted explicitly here because they are clearly visible in the objective and variable values. Again, two CRs are discovered: CR_0, containing the baseline scenario, corresponds to parameter realizations where ISRU output is low and/or maintenance requirements are high; the other, CR_1, occurs when maintenance requirements are low and output is high.

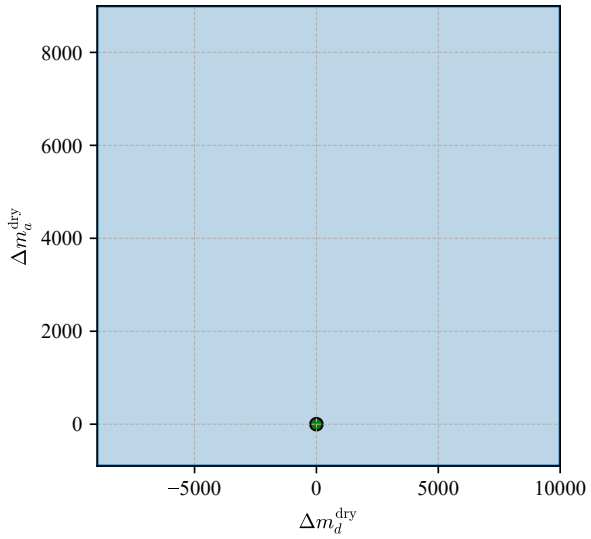

Fig. 6. CR of Case Study 2. The green point indicates the parameter values for which Eq. mpLP2 was solved. The blue region CR_0 encompasses the entire parameter space.

CR_0 represents the decision to not launch any ISRU infrastructure. Crossing from CR_0 into CR_1 represents a discrete change in the pre-deployment plan, with ISRU infrastructure and associated maintenance supplies being launched in the pre-deployment stage. Further, the results provide the continuous variation in the ISRU infrastructure required as the parameter realizations vary with CR_1.

The limit of CR_1 as the maintenance requirements go to zero could be considered an edge case. Whilst still a valid set of active constraints for CR_1, the decision to launch no maintenance supplies makes the non-negativity constraint on m^{m} active also. Consequently, we observe some "noise" in the optimal variable values, specifically, in m_0^{s} and m_1^{s}. The decision to launch crew supplies with the pre-deployment mission or with the crew themselves becomes equivalent, so the linear algebra solver inconsistently chooses one solution or the other.

6. Discussion

The results of these case studies provide useful information for a potential mission architect. Under the baseline system parameter values, we found that ISRU infrastructure does not feature in an optimal mission design, but, with sufficiently high product output, becomes a part of the optimal design. This allows the program manager to make decisions regarding ISRU technology development,

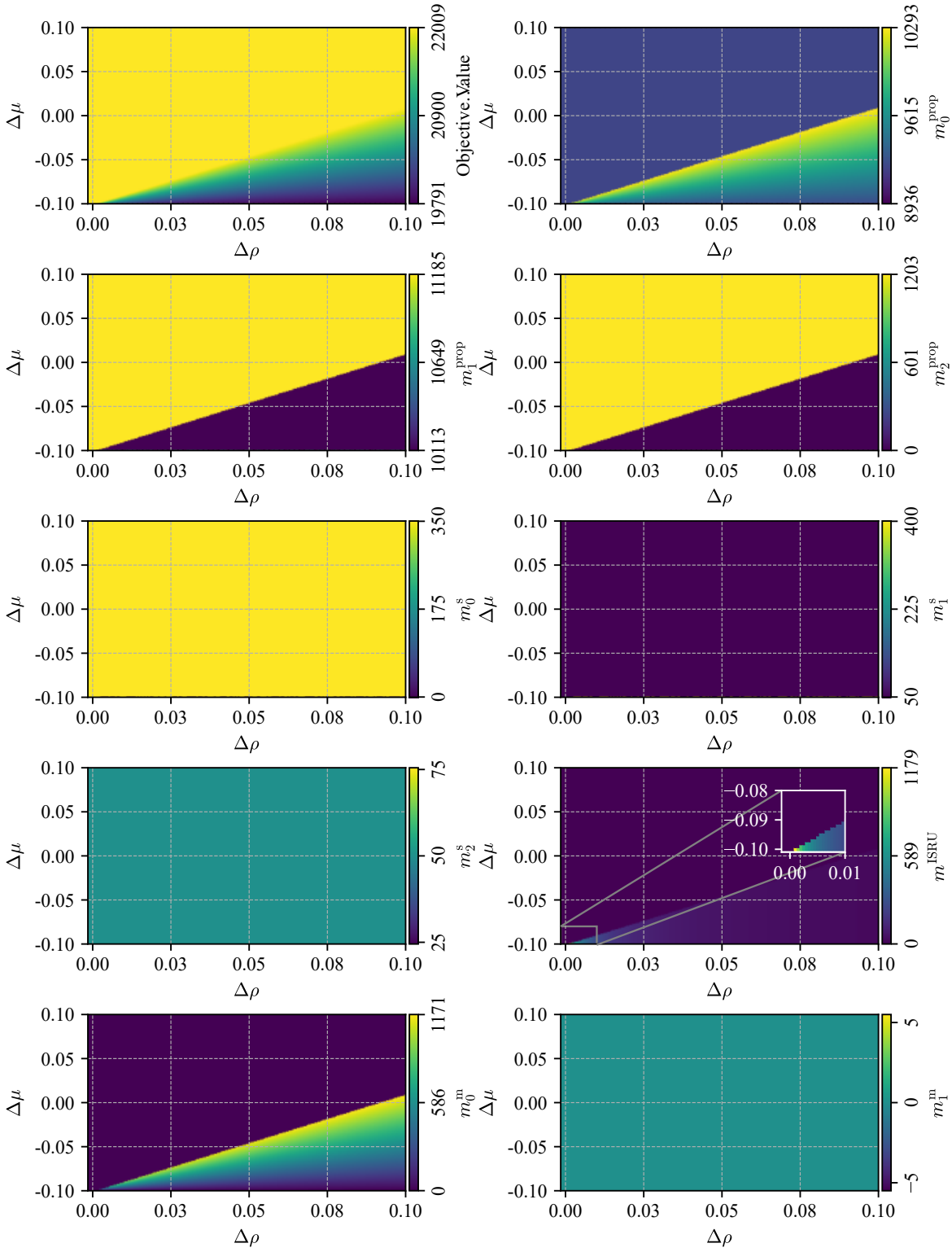

Fig. 7. Objective and variable values as functions of the LHS-parameters of Case Study 3.

and to set minimum output requirements in the case that they decide to pursuit the technology development activity.

Conversely, we found that vehicle dry masses do not affect the discrete, program-level decisions, and so the program manager does not need to place any mass limitation requirements on the vehicle design.

In addition to establishing the parameter boundaries at which the high-level, discrete decisions change, this method also tells the program manager how mission design variables change continuously *within* those bounds. For example, within the critical region where ISRU usage is optimal, the method tells us how much infrastructure to deploy depending on performance of the infrastructure.

7. Conclusions

This paper has presented an application of multi-parametric programming methods for the identification of critical system and mission parameters in future space mission design. In particular, this work has demonstrated how mpLP methods can be used for informing the high-level, discrete decisions that mission managers must make in the early stages of architecture design, and when setting system requirements prior to system design and technology development.

Considering the prevalence of integers variables in space mission design, future work should focus on integrating integer variables into parametric programming. Wittmann-Hohlbein and Pistikopoulos developed a number of approximate techniques [32–34] for achieving this, but generalisable and exact methods appear to be an area of ongoing research.

Acknowledgements

This material is based upon work supported by the National Science Foundation under Grant: 1942559.

References

[1] P. T. Grogan, A. Siddiqi, and O. L. De Weck, "Matrix methods for optimal manifesting of multinode space exploration systems," *Journal of Spacecraft and Rockets*, vol. 48, no. 4, pp. 679–690, 2011, ISSN: 0022-4650, 1533-6794. DOI: 10.2514/1.51870.

[2] T. Ishimatsu, O. L. de Weck, J. A. Hoffman, Y. Ohkami, and R. Shishko, "Generalized multicommodity network flow model for the earth–moon–mars logistics system," *Journal of Spacecraft and Rockets*, vol. 53, no. 1, pp. 25–38, 2016, ISSN: 0022-4650, 1533-6794. DOI: 10.2514/1.A33235.

[3] K. Ho, O. de Weck, J. Hoffman, and R. Shishko, "Dynamic modeling and optimization for space logistics using time-expanded networks," *Acta Astronautica*, vol. 105, 2014. DOI: 10.1016/j.actaastro.2014.10.026.

[4] D. C. Arney and A. W. Wilhite, "Modeling space system architectures with graph theory," en, *Journal of Spacecraft and Rockets*, vol. 51, no. 5, pp. 1413–1429, 2014, ISSN: 0022-4650, 1533-6794. DOI: 10.2514/1.A32578.

[5] N. Gollins and K. Ho, "Hierarchical framework for space exploration campaign schedule optimization," *Journal of Spacecraft and Rockets*, vol. 61, no. 5, 2024. DOI: https://doi.org/10.2514/1.A35828. [Online]. Available: https://arc.aiaa.org/doi/10.2514/1.A35828?Site=aiaa_frame.

[6] M. Salmaso, Z. Wang, L. Dueñas-Osorio, and M. Jernigan, "Sustainable space logistics for artemis missions and deep space exploration," in *AIAA SciTech Forum 2025*, Orlando, FL, 2025.

[7] H. Chen and K. Ho, "Integrated space logistics mission planning and spacecraft design with mixed-integer nonlinear programming," *Journal of Spacecraft and Rockets*, vol. 55, no. 2, pp. 365–381, 2018, ISSN: 0022-4650, 1533-6794. DOI: 10.2514/1.A33905.

[8] H. Chen, T. Sarton Du Jonchay, L. Hou, and K. Ho, "Integrated in-situ resource utilization system design and logistics for mars exploration," *Acta Astronautica*, vol. 170, pp. 80–92, 2020, ISSN: 00945765. DOI: 10.1016/j.actaastro.2020.01.031.

[9] H. Chen, T. Sarton du Jonchay, L. Hou, and K. Ho, "Multifidelity space mission planning and infrastructure design framework for space resource logistics," *Journal of Spacecraft and Rockets*, vol. 58, no. 2, pp. 538–551, Mar. 2021, ISSN: 0022-4650, 1533-6794. DOI: 10.2514/1.A34666.

[10] M. Isaji, Y. Takubo, and K. Ho, "Multidisciplinary design optimization approach to integrated space mission planning and spacecraft design," *Journal of Spacecraft and Rockets*, vol. 59, no. 5, pp. 1660–1670, Nov. 2021. DOI: 10.2514/1.A35284.

[11] C. Downs, B. E. Robertson, and D. N. Mavris, "A taxonomy of uncertainty for space exploration campaigns," in *ASCEND 2022*, Las Vegas, Nevada Online: American Institute of Aeronautics and Astronautics, 2022, ISBN: 978-1-62410-662-0. DOI: 10.2514/6.2022-4333. [Online]. Available: https://arc.aiaa.org/doi/10.2514/6.2022-4333.

[12] M. Isaji and K. Ho, "Integrated space mission planning under uncertainty via stochastic and decomposition-based optimization," in *AIAA Aviation Forum and ASCEND*, 2024.

[13] Y. Takubo, H. Chen, and K. Ho, "Hierarchical reinforcement learning framework for stochastic spaceflight campaign design," *Journal of Spacecraft and Rockets*, vol. 59, no. 2, pp. 421–433, 2022. DOI: 10.2514/1.A35122.

[14] H. Chen, B. M. Gardner, P. T. Grogan, and K. Ho, "Flexibility management for space logistics via decision rules," *Journal of Spacecraft and Rockets*, vol. 58, no. 5, pp. 1314–1324, 2021, ISSN: 0022-4650, 1533-6794. DOI: 10.2514/1.A34985.

[15] N. J. Gollins and K. Ho, "Optimization of multi-mission space exploration campaign schedules subject to stochastic launch delay," in *AIAA SCITECH Forum*, Orlando, FL: American Institute of Aeronautics and Astronautics, 2024, ISBN: 978-1-62410-711-5. DOI: 10.2514/6.2024-2718. [Online]. Available: https://arc.aiaa.org/doi/10.2514/6.2024-2718.

[16] W. J. O'Neill and D. A. Delaurentis, "Assessing program-level objectives of space exploration architectures using portfolio-optimization methods," *Journal of Spacecraft and Rockets*, vol. 58, no. 5, pp. 1248–1262, 2021, ISSN: 0022-4650, 1533-6794. DOI: 10.2514/1.A34762.

[17] T. Gal, *Postoptimal Analyses, Parametric Programming, and Related Topics: Degeneracy, Multicriteria Decision Making, Redundancy*. Walter de Gruyter, 2010, ISBN: 978-3-11-087120-3.

[18] T. Gal and J. Nedoma, "Multiparametric linear programming," *Management Science*, vol. 18, no. 7, pp. 406–422, 1972, ISSN: 0025-1909, 1526-5501. DOI: 10.1287/mnsc.18.7.406.

[19] R. Khalilpour and I. Karimi, "Parametric optimization with uncertainty on the left hand side of linear programs," *Computers Chemical Engineering*, vol. 60, pp. 31–40, 2014, ISSN: 00981354. DOI: 10.1016/j.compchemeng.2013.08.005.

[20] F. Borrelli, A. Bemporad, and M. Morari, "Geometric algorithm for multiparametric linear programming," *Journal of Optimization Theory and Applications*, vol. 118, no. 3, pp. 515–540, 2003, ISSN: 0022-3239, 1573-2878. DOI: 10.1023/B:JOTA.0000004869.66331.5c.

[21] C. Jones, E. Kerrigan, and J. Maciejowski, "Lexicographic perturbation for multiparametric linear programming with applications to control," *Automatica*, vol. 43, no. 10, pp. 1808–1816, 2007, ISSN: 00051098. DOI: 10.1016/j.automatica.2007.03.008.

[22] P. Ahmadi-Moshkenani, T. A. Johansen, and S. Olaru, "On degeneracy in exploration of combinatorial tree in multi-parametric quadratic programming," in *2016 IEEE 55th Conference on Decision and Control (CDC)*, 2016, pp. 2320–2326. DOI: 10.1109/CDC.2016.7798609. [Online]. Available: https://ieeexplore.ieee.org/document/7798609/.

[23] A. Akbari and P. I. Barton, "An improved multiparametric programming algorithm for flux balance analysis of metabolic networks," *Journal of Optimization Theory and Applications*, vol. 178, no. 2, pp. 502–537, 2018, ISSN: 0022-3239, 1573-2878. DOI: 10.1007/s10957-018-1281-x.

[24] H. Liu, Y. Guo, and H. Liu, "On degeneracy issues in multi-parametric programming and critical region exploration based distributed optimization in smart grid operations," *CSEE Journal of Power and Energy Systems*, pp. 1–14, 2025, ISSN: 2096-0042. DOI: 10.17775/CSEEJPES.2023.07470.

[25] A. Einstein, "Die grundlage der allgemeinen relativitätstheorie," *Annalen der Physik*, vol. 354, no. 7, pp. 769–822, 1916, ISSN: 1521-3889. DOI: 10.1002/andp.19163540702.

[26] E. N. Pistikopoulos, N. A. Diangelakis, and R. Oberdiek, *Multi-Parametric Optimization and Control*. Hoboken, NJ: Wiley, 2021, ISBN: 9781119265184. DOI: 10.1002/9781119265245.

[27] K. Fukuda, *cdd/cdd+ Reference Manual*, 2021. [Online]. Available: https://people.inf.ethz.ch/fukudak/cdd_home/cddlibman2021.pdf.

[28] M. C. M. Troffaes, *pycddlib Documentation*, 2025. [Online]. Available: https://pycddlib.readthedocs.io/en/stable/.

[29] V. M. Charitopoulos, L. G. Papageorgiou, and V. Dua, "Multi-parametric linear programming under global uncertainty," *AIChE Journal*, vol. 63, no. 9, pp. 3871–3895, 2017, ISSN: 0001-1541, 1547-5905. DOI: 10.1002/aic.15755.

[30] A. Ben-Israel and T. N. E. Greville, *Generalized Inverses: Theory and Applications* (CMS Books in Mathematics), 2nd ed. New York: Springer-Verlag, 2003, ISBN: 978-0-387-00293-4. DOI: 10.1007/b97366. [Online]. Available: http://link.springer.com/10.1007/b97366.

[31] S. S. Schreiner, L. Sibille, J. A. Dominguez, and J. A. Hoffman, "A parametric sizing model for molten regolith electrolysis reactors to produce oxygen on the moon," *Advances in Space Research*, vol. 57, no. 7, pp. 1585–1603, 2016, ISSN: 02731177. DOI: 10.1016/j.asr.2016.01.006.

[32] M. Wittmann-Hohlbein and E. N. Pistikopoulos, "A two-stage method for the approximate solution of general multiparametric mixed-integer linear programming problems," *Industrial Engineering Chemistry Research*, vol. 51, no. 23, pp. 8095–8107, 2012, ISSN: 0888-5885. DOI: 10.1021/ie201408p.

[33] M. Wittmann-Hohlbein and E. N. Pistikopoulos, "On the global solution of multi-parametric mixed integer linear programming problems," *Journal of Global Optimization*, vol. 57, no. 1, pp. 51–73, 2013, ISSN: 0925-5001, 1573-2916. DOI: 10.1007/s10898-012-9895-2.

[34] M. Wittmann-Hohlbein and E. N. Pistikopoulos, "Approximate solution of mp-milp problems using piecewise affine relaxation of bilinear terms," *Computers Chemical Engineering*, vol. 61, pp. 136–155, 2014, ISSN: 00981354. DOI: 10.1016/j.compchemeng.2013.10.009.